

CHANGES IN MICROSTRUCTURE AND PROPERTIES OF AUSTENITIC STEEL AISI 316 DURING HIGH-PRESSURE TORSION

Andrey Volokitin¹, Abdrakhman Naizabekov², Irina Volokitina², Alexandr Kolesnikov³

¹Karaganda State Industrial University
101400, Republic av. 30, Temirtau, Kazakhstan

²Rudny Industrial Institute, 111500
50 let Oktyabrya str. 38, Rudny, Kazakhstan

³M. Auezov South Kazakhstan University, 160009
D. Erimbetov str., 38/32, Shymkent, Kazakhstan
E-mail: irinka.vav@mail.ru

Received 08 February 2022

Accepted 20 March 2022

ABSTRACT

The effect of high-pressure torsion process in a new die on the structure and mechanical properties of corrosion-resistant steel AISI 316 was studied. Deformation was carried out at room temperature, the number of deformation cycles was 7. In the process of high-pressure torsion, the structure of samples is considerably refined to nanostructured, so steel AISI 316 with an average grain size of 30 μm after deformation is refined to 80 - 100 nm. The tensile strength and yield strength values increase in seven passes from 595 to 1590 MPa and from 320 to 870 MPa, respectively. Relative elongation changes from 55 to 25 %, but remains at a sufficient level for an application. The initial structure of non-deformed steel has good ductility and demonstrates typical signs of ductile fracture. But with increasing HPT cycles the fracture mechanism changes from ductile to brittle, indicating a decrease in ductility of stainless steel AISI 316.

***Keywords:** high-pressure torsion, microstructure, austenitic steel, metal, severe plastic deformation.*

INTRODUCTION

In the last twenty years, there is an increasing interest in bulk nanocrystalline materials, and especially in materials processed by severe plastic deformation (SPD) methods [1 - 5], such as high pressure torsion (HPT) [6 - 8] and angular equal channel pressing (ECAP) [9 - 12]. They are successfully used as new processing technologies to obtain nano- and submicrocrystalline metal materials. This interest is due not only to the unique physical and mechanical properties achieved by various nanostructured materials, but also to a number of material advantages over other nanostructured materials. When implementing SPD methods, grain refinement occurs during processing due to shear deformations and phase transformations [13, 14]. This results in ultrafine grain size and unique chemical, physical, and mechanical properties, such as high yield strength and tensile strength, significantly higher than those of the coarse-grained state [15 - 17].

As a result of its ability to strongly deform the sample (true deformation ≥ 10) and to achieve excellent grain refinement with exceptional strength, the HPT method, which involves treating the sample by torsional deformation under pressure and compression, has become very important and one of the main SPD methods [6 - 8]. Although extensive research has been done in this area, the behavior and fundamental principles are not yet fully understood because such materials have extraordinary strength, but ductility is too low, and also discs treated in this way have anisotropic properties between the center and the edges [18].

Today, with SPD capabilities to produce bulk nanostructured materials, the use of such materials in electrical wires and microdevices is very realistic. In the field of biomedical engineering bulk nanostructured materials have already been successfully used as materials for dental implants. This opens the door for transition of researches to commercial production of a wide range of promising products.

In order to be able to develop new and innovative material processing methods that can improve the performance and mechanical properties of the materials processed by SPD, a thorough understanding of the mechanisms of formation and evolution of microstructure and grain refinement, as well as the physics of deformation and fracture, is required.

Based on the above, the purpose of this study was to investigate the evolution of the microstructure and the mechanism of grain refinement during deformation and also to determine the factors influencing on grain refinement during deformation.

One of the stages of the study was the development of a special die design, which allows to implement this process of intense plastic deformation on ring workpieces. On the basis of modeling in the software package Deform, given in papers [19, 20], design drawings were developed. The design consists of several parts: an upper striker which is driven by the press; a lower striker which is driven by the translational motion of the upper striker and a matrix. On the lower edge of the upper striker 4 periodic spiral shaped indentations are created. In the center of the upper striker there is a cylindrical hole for the rod of deforming element and for ensuring alignment of both strikers. The lower striker has

several steps. This design solution is necessary because in this case we are talking about deformation of a circular workpiece, but not of a disk workpiece (Fig. 1).

EXPERIMENTAL

The initial workpiece had a ring shape with a diameter of 76 mm, a width of 3.5 mm and a thickness of 3 mm. Austenitic stainless steel AISI 316 (0.08 % C; 13 % Ni; 17 % Cr; 2.0 % Mo; 0.6 % Si; 1.8 % Mn; 0.8 % Ti) was selected as the material of the workpiece because it is high-strength, corrosion-resistant, ductile and heat-resistant. The advantages of the steel are the addition of molybdenum and a higher content of chromium and nickel.

The main purpose of preheating of workpieces in our case is to obtain a fine-grained structure and to reduce the force during deformation, which will help to carry out further operation - HPT without much effort and losses, as well as to obtain in the future an ultrafine-grained structure. It is well known that the initial microstructure affects the microstructure hardening process during HPT, since a more homogeneous initial microstructure will result in a more homogeneous final microstructure and therefore better mechanical properties. Thus, an initial

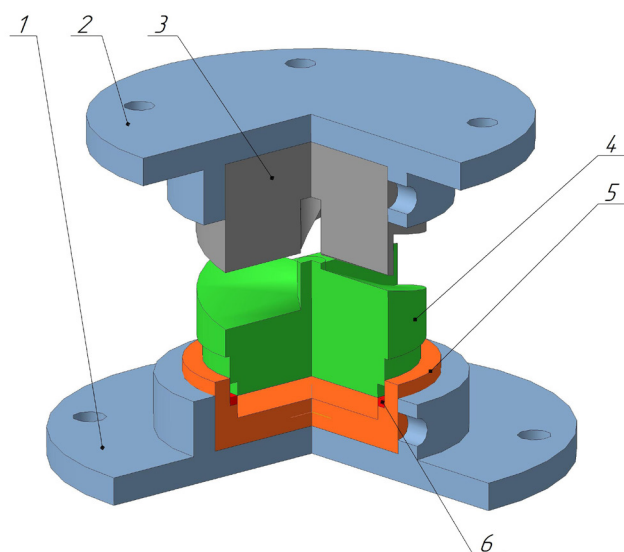


Fig. 1. General view of the complete construction: 1 - bottom carrier, 2 - top carrier, 3 - upper striker, 4 - lower striker, 5 - matrix, 6 - piston ring.

heat treatment was applied to the supplied ferrite-perlite microstructure to modify it to a more homogeneous. To obtain a single-phase γ - structure in our steel we apply a standard heat treatment, which includes heating to a temperature of 1100°C, holding for 30 min and cooling in water. As a result of such heat treatment in chromium-nickel corrosion-resistant steels γ - solid solution with a homogeneous distribution of alloying elements is fixed, in which there are no carbide precipitations, which provides the best corrosion properties [21].

The deformation temperature should be lower than 0.4 T_m . At this temperature, no recrystallization processes occur, so the main deformation mechanism will be the movement of dislocations. At higher deformation temperatures, alternative mechanisms, such as dislocation annihilation and diffusion creep, will be activated, which will have a negative effect on grain refinement. Thus, the room temperature was chosen as deformation temperature.

The laboratory experiment was carried out on a crank hot-stamping single-column press with the force of 1000 kN model PB 6330-02. Deformation was carried out at room temperature, since in austenitic steels martensitic transformation is observed and, depending on the deformation temperature, the amount of martensite in the structure can vary. The number of deformation cycles was 7. Experimental tooling for the HPT was made of 5XV2C steel on a CNC turn-mill machine. The components of the structure were subjected to a special heat treatment after manufacturing to increase the strength properties. After manufacturing all elements of the structure were assembled. Thus, the lower holder was installed on the base plate of the hydraulic press and secured with tie bolts through the retaining brackets (Fig. 2). The lower striker was installed in the bottom holder, with a chamber for deformation of rings, the upper matrix was installed from above on the sample.

Metallographic analysis of all examined samples in cross-sectional and longitudinal sections was performed using a JEM2100 electron transmission microscope. All samples were tested in the median plane to avoid the influence of peripheral areas. Preparation of samples for metallographic analysis was carried out on an electrolytic sample preparation unit Struers.

Mechanical uniaxial tension tests were performed at room temperature on Instron 5882 machine at a deformation rate of 1.0 mm min⁻¹. The sample

deformation was measured with an Instron strain gauge. Tensile tests were carried out on flat samples cut from the ring (working part dimensions 3.0 x 3.0 x 6.0 mm) in accordance with GOST 1497-84 recommendations. Tensile tests of mechanical properties were used to determine strength and ductility characteristics: yield strength ($\sigma_{0.2}$), tensile strength (σ_B) and maximum elongation to failure (δ).

Vickers microhardness was determined using DM-8 automatic microhardness tester (Affri).

RESULTS AND DISCUSSION

Fig. 3(a) shows that the microstructure before HPT is coarse-grained, with an average grain size of 30 μ m. In the structure of metastable austenitic steel AISI 316 in the initial state contains \approx 100 % austenite, polyhedral grains with thin boundaries and annealing twins.

After 1 cycle of deformation, deformation twins appear in austenite (Fig. 3(b)). When the number of cycles increases to 2, the number of dislocations near the grain boundaries increases, since the boundaries are a barrier to dislocation motion. After 3 cycles of deformation, the austenite structure shows a large number of dislocation



Fig. 2. Construction assembly.

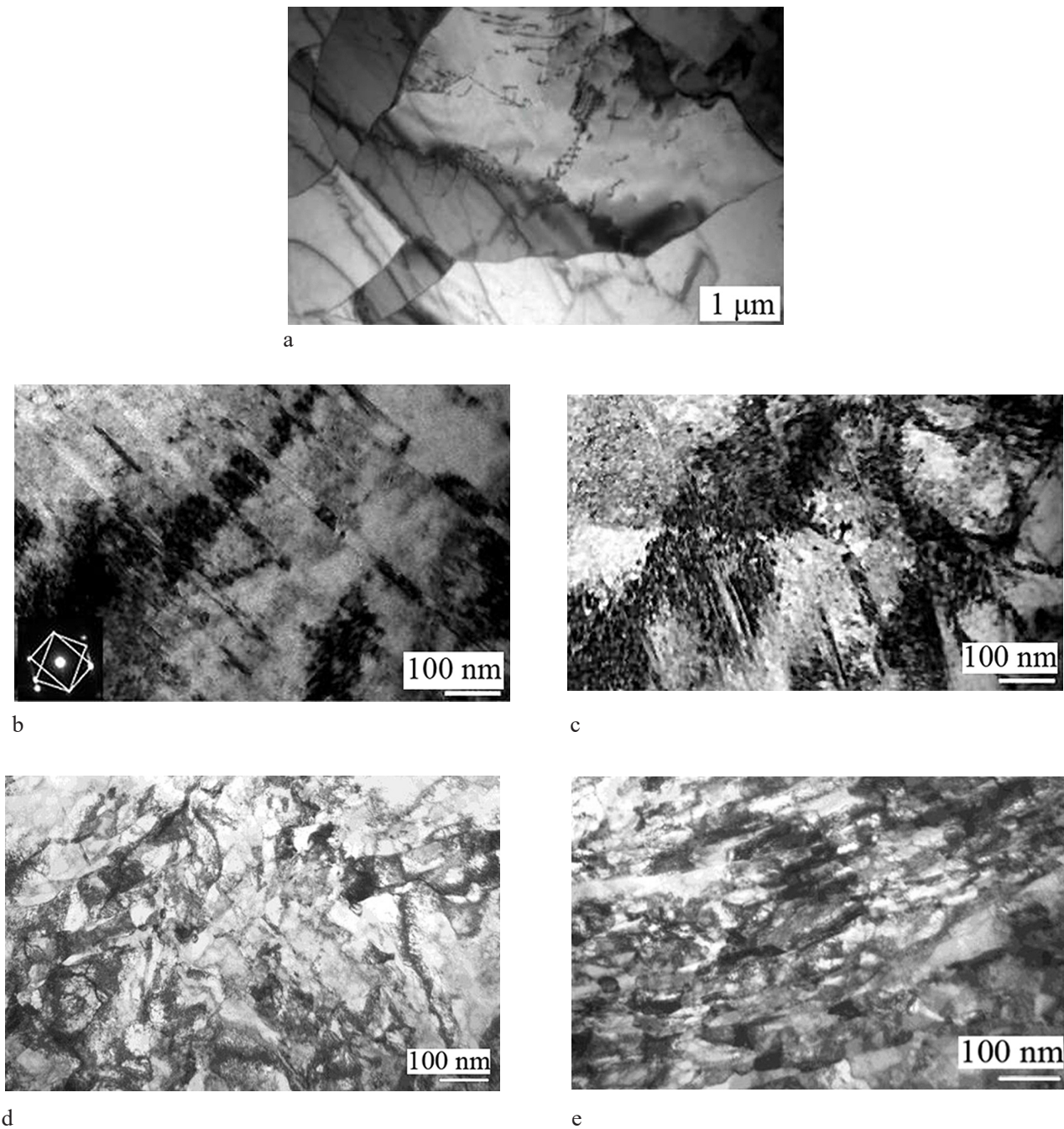


Fig. 3. Microstructure of AISI 316 steel during high-pressure torsion: a - initial state; b - 1 cycle; c - 3 cycles; d - 5 cycles; e - 7 cycles.

accumulations adjacent to deformation twins, which suggests a mixed deformation mechanism including deformation twinning and dislocation sliding during HPT (Fig. 3(c)). In austenite, because of the high level of packing defect energy, many deformation dislocations annihilate and others rearrange into dislocation cells and then turn into grains with grain boundaries with large

misorientation angles. As the number of cycles increases to 5, the size of austenite grains decreases even further to 0.3 μm , as shown in Fig. 3(d), shear bands appear in the austenite, and the boundaries of twins become less clearly delineated. In accordance with the literature data, twins are suitable for the nucleation of α -martensite, as well as for $\gamma \rightarrow \alpha$ -transformation [22]. It is also known

that the shear $\gamma \rightarrow \alpha'$ phase transformation in the cold deformation temperature intervals develops when the critical deformation degree is reached during large plastic deformation in materials with low packing defect energy. This deformation mechanism is considered as one of the mechanisms of structure formation of nanocrystalline and submicrocrystalline structures during large plastic deformation in materials with low energy of packing defects. After 7 deformation cycles, ($\gamma \rightarrow \alpha$)-martensitic transformation and formation of an insignificant fraction of α -martensite occur (Fig. 3(e)). Increasing the degree of deformation leads to an increase in the volume fraction of α -martensite in the phase transformation up to 27 %, but the intensity of martensitic transformation decreases with increasing deformation.

In addition to investigated changes in steel microstructure during deformation, the mechanical properties of the rings were studied during tensile. As shown by mechanical tensile tests, obtained in the process of HPT, nanocrystalline structure of steel AISI 316 has a high complex of mechanical properties in contrast to the initial state where the steel shows low strength properties

ultimate strength - 595 MPa, yield strength - 320 MPa with fairly high ductility characteristics 55 %. It can be seen that the formation of nanocrystalline structure after 7 cycles of deformation by HPT method with an average grain size of 80 - 100 nm leads to an increase in the yield strength from 320 to 870 MPa compared to the initial state. The strength increases from 595 to 1590 MPa in accordance with the decrease in grain size and coherent scattering regions and the increase in microdeformation values. The plasticity value decreases sharply compared to the initial state up to 25 %, but remains at a sufficient level for an application.

The results of microhardness determination correlate with the data of mechanical tests and testify that the HPT in the new die allows obtaining sufficiently homogeneous hardness over the entire cross section of the ring. After seven passes of HPT the microhardness in comparison with an initial condition increases approximately 3 times from 1080 MPa to 2680 MPa. In this case, the main increase in hardness falls on the first 4 passes to 40 %.

Fig. 4 shows photographs of AISI 316 stainless steel after tensile testing. The resulting undeformed steel initial sample shows a feature of the sample neck, with the shear

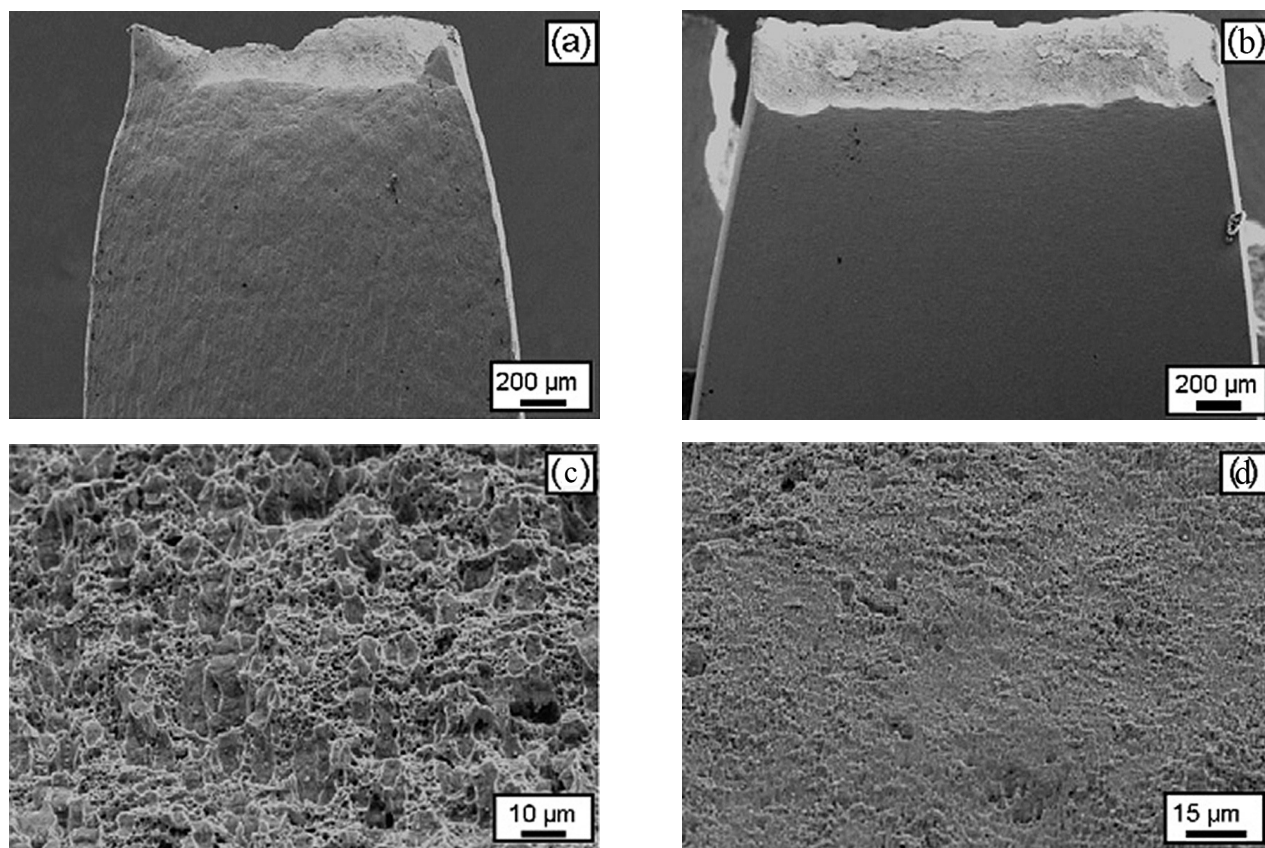


Fig. 4. Fractography of AISI 316 steel after tensile: a, c - initial state; b, d - 7 cycles.

edge formed around the fracture surface, as shown in Fig. 4(a). The grains are elongated along the tensile axis, indicating high tensile ductility. Within the elongated grains, there are several shear bands perpendicular to the fracture plane, which is the result of neck deformation. After 7 HPT cycles, the sample has a small neck and the fracture surface is almost flat (Fig. 4(b)).

Clear bands of longitudinal shear appear on the lateral surface, caused by neck deformation. This indicates that the sample has a weak neck on the lateral surface. Under high magnification, it is clearly visible that the fracture surface of the undeformed sample contains many deep depressions, uniformly distributed like honeycombs (Fig. 4(c)). After 7 passes of deformation, small depressions appear only in local areas, and on the fracture surface of the sample, there are many smooth areas (Fig. 4(d)).

From the results it can be concluded that the initial structure of non-deformed steel has good ductility and demonstrates typical signs of ductile fracture. But with increasing HPT cycles the fracture mechanism changes from ductile to brittle which indicates a decrease in ductility of stainless steel 08X17H13M2.

CONCLUSIONS

The results of the study showed that in the process of HPT the structure of samples is significantly refined to nanostructured, so deformation of AISI 316 steel with an average grain size of 30 μm leads to the formation of uniform microstructure of 50 - 60 nm, consisting of a mixture of austenite and α - martensite. The formation of nanostructured state in the process of high-pressure torsion in a new die at room temperature occurs through the action of two mechanisms. The first mechanism is related to the fragmentation of initial grains due to the formation of deformation shear bands and deformation twins, and the second mechanism is related to the development of $\gamma \rightarrow \alpha$ phase transformation by the shear mechanism of deformation martensite formation. The tensile strength and yield strength values increase in seven passes from 595 to 1590 MPa and from 320 to 870 MPa, respectively. Relative elongation changes from 55 to 25 %, but remains at a sufficient level for the application.

Acknowledgements

This research was funded by the Science Committee of the Ministry of Education and Science of the Republic of Kazakhstan (Grant No. AP08856353).

REFERENCES

1. M. Polyakova, A. Gulin, D. Constantinov, Investigation of microstructure and mechanical properties of carbon steel wire after continuous method of deformational nanostructuring, *Appl. Mechan. Mater.*, 436, 2013, 114-120.
2. E.P. Orlova, G.G. Kurapov, I. Volokitina, A. Turdaliev, Plasticity as a physical-chemical process of deformation of crystalline solids. *J. Chem. Technol. Metall.*, 51, 4, 2016, 451-457.
3. K. Muszka, D. Zych, P. Lisiecka-Graca, L. Madej, Ja. Majta, Experimental and Molecular Dynamic Study of Grain Refinement and Dislocation Substructure Evolution in HSLA and IF Steels after Severe Plastic Deformation, *Metals*, 10, 2020, 1122.
4. R. Mythili, R.K. Irana, L. Herojit Singh, R. Govindaraj, A. Sinha, M. Singh, S. Saroja, M. Vijayalakshmi, M. Deb, Identification of Retained Austenite in 9Cr-1.4W-0.06Ta-0.12C Reduced Activation Ferritic Martensitic Steel, *Symmetry*, 14, 2, 2022, 196.
5. A. Naizabekov, I. Volokitina, Effect of the Initial Structural State of Cr-Mo High-Temperature Steel on Mechanical Properties after Equal-Channel Angular Pressing. *Phys. Met. Metallogr.*, 120, 2019, 177-183.
6. A.P. Zhilyaev, G. Ringot, Yi.Huang, J.M.Cabrera, T.G. Langdon, Mechanical behavior and microstructure properties of titanium powder consolidated by high-pressure torsion, *Mater. Sci. Eng. A*, 688, 2017, 498-504.
7. M. Kawasaki, B. Ahn, H.J. Lee, A.P. Zhilyaev, T.G. Langdon, Using high-pressure torsion to process an aluminum-magnesium nanocomposite through diffusion bonding. *J. Mater. Res*, 31, 2015, 88-99.
8. A. Volokitin, A. Naizabekov, I. Volokitina, S. Lezhnev, E. Panin, Thermomechanical treatment of steel using severe plastic deformation and cryogenic cooling, *Mater. Lett.*, 304, 2021, 130598.
9. E.I. Fakhretdinova, G.I. Raab, R.Z. Valiev, Modeling of Metal Flow during Processing by Multi-ECAP-Conform, *Adv. Eng., Materials*, 17, 12, 2015, 1723-1727.
10. A.V. Polyakov, I.P. Semenova, G.I. Raab, Peculiarities of ultrafine-grained structure formation in Ti Grade-4 using ECAP-Conform, *Adv. Mater. Sci.*, 31, 1, 2012, 78-84.

11. U. Chakkingal, A. Suriadi, P. Thomson, The development of microstructure and the influence of processing route during equal channel angular drawing of pure aluminum, *Mater. Sci. Eng. A*, 266, 1999, 241-249.
12. I. Volokitina, G. Kurapov, Effect of Initial Structural State on Formation of Structure and Mechanical Properties of Steels Under ECAP, *Metal Science and Heat Treatment*, 59, 2018, 786-792.
13. Wei-Jen Cheng, Chaur-Jeng Wang, Study of microstructure and phase evolution of hot-dipped aluminide mild steel during high-temperature diffusion using electron backscatter diffraction, *Appl. Surf. Sci.*, 257, 2011, 4663-4668.
14. D.P. Verma, Sh.A. Pandey, A. Bansal, Sh. Upadhyay, N.K. Mukhopadhyay, G.V.S. Sastry, R. Manna, Bulk Ultrafine-Grained Interstitial-Free Steel Processed by Equal-Channel Angular Pressing Followed by Flash Annealing. *J. Mater. Eng. Perform.*, 25, 2016, 5157-5166.
15. I. Volokitina, Structure and mechanical properties of aluminum alloy 2024 after cryogenic cooling during ECAP, *J. Chem. Technol. Metall.*, 55, 3, 2020, 580-585.
16. R.Z. Valiev, R.K. Islamgaliev, I.V. Alexandrov, Bulk nanostructured materials from severe plastic deformation, *Prog. Mater. Sci.*, 45, 2000, 103-189.
17. A. Boikov, V. Payor, R. Savelev, A. Kolesnikov, Synthetic Data Generation for Steel Defect Detection and Classification Using Deep Learning, *Symmetry*, 13, 7, 2021, 1176.
18. A.P. Zhilyaev, T.G. Langdon, Using high-pressure torsion for metal processing: Fundamentals and applications. *Prog. Mater. Sci.*, 53, 2008, 893-979.
19. A. Volokitin, I. Volokitina, E. Panin, A. Naizabekov, S. Lezhnev, Strain state and microstructure evolution of AISI-316 austenitic stainless steel during high-pressure torsion (HPT) process in the new stamp design, *Metalurgija*, 60, 3-4, 2021, 325-328.
20. A.V. Volokitin, A.B. Naizabekov, I.E. Volokitina, E.A. Panin, G.J. Moldabaeva, Stamp design for the implementation of torsion under high pressure, *Bulletin of Kazntu*, 2, 2021, 207-214, (in Russian).
21. M.I. Goldstein, S.V. Grachev, Yu.G. Veksler, Special steels. Textbook for universities, M: Metallurgy, 1985. (in Russian).
22. J. Su, D. Raabe, Z. Li, Hierarchical microstructure design to tune the mechanical behavior of an interstitial TRIP-TWIP high-entropy alloy, *Acta Materialia*, 163, 2019, 40-54.